

X-ray phase imaging of a packaged IC chip using X-ray array source

Y. Park and J. Choi^{a)}

Department of Physics, Dankook University

29 Anseo-Dong, Cheonan, 330–714, Korea

a) choi@dankook.ac.kr

Abstract: We have developed a novel configuration of an X-ray grating interferometer for the phase imaging of a packaged IC chip. A square source grating is used, and a beam splitter and an analyzer grating are positioned downstream of the investigated sample. In the proposed method, the period of source grating is smaller than the last of two gratings, the configuration of which could be implemented for phase imaging. Phase images retrieved using the principle of in-line phase contrast imaging and phase detection are the phase stepping method used in the X-ray grating interferometer. The wrapped phase images of the packaged IC chip are obtained from nine Moiré fringe patterns, using an exposure time of 34 ms for each scan.

Keywords: X-ray phase imaging, X-ray interferometer, warp phase map, IC chip imaging

Classification: Electron tubes, vacuum and beam technology

References

- [1] F. Pfeiffer, M. Bech, O. Bunk, P. Kraft, E. F. Eikenberry, C. Brönnimann, C. Grünzweig, and C. David, “Hard-X-ray dark-field imaging using a grating interferometer,” *Nature Materials*, vol. 7, pp. 134–137, Jan. 2008.
- [2] A. Momose, W. Yashiro, Y. Takeda, Y. Suzuki, and T. Hattori, “Phase Tomography by X-ray Talbot Interferometry for Biological Imaging,” *Jpn. J. Appl. Phys.*, vol. 45, no. 6A, pp. 5254–5262, June 2006.
- [3] F. Pfeiffer, T. Weitkamp, O. Bunk, and C. David, “Phase retrieval and differential phase-contrast imaging with low-brilliance X-ray sources,” *Nature Phys.*, vol. 2, pp. 258–261, March 2006.
- [4] A. Momose, S. Kawamoto, I. Koyama, Y. Hamaishi, K. Takai, and Y. Suzuki, “Demonstration of X-Ray Talbot Interferometry,” *Jpn. J. Appl. Phys.*, vol. 42, no. 7B, pp. L866–L868, July 2003.
- [5] Y. I. Nesterets, S. W. Wilkins, T. E. Gureyev, A. Pogany, and A. W. Stevenson, “On the optimization of experimental parameters for x-ray in-line phase-contrast imaging,” *Rev. Sci. Instrum.*, vol. 76, no. 9, pp. 093706-1–093706-15, Sept. 2005.
- [6] X. Wu, H. Liu, and A. Yan, “Optimization of X-ray phase-contrast imaging based on in-line holography,” *Nucl. Instr. and Meth. Phys. Res. B*, vol. 234, no. 4, pp. 563–572, July 2005.

- [7] T. J. Davis, D. Gao, T. E. Gureyev, A. W. Stevenson, and S. W. Wilkins, “Phase-contrast imaging of weakly absorbing materials using hard X-rays,” *Nature*, vol. 373, pp. 595–598, Feb. 1995.
- [8] E. Pagot, P. Cloetens, S. Fiedler, A. Bravin, P. Coan, J. Baruchel, J. Härtwig, and W. Thomlinson, “A method to extract quantitative information in analyzer-based x-ray phase contrast imaging,” *Appl. Phys. Lett.*, vol. 82, pp. 3421–3423, May 2003.
- [9] X. Wu and H. Liu, “Clarification of aspects in in-line phase-sensitive x-ray imaging,” *Med. Phys.*, vol. 34, no. 2, pp. 737–743, Feb. 2007.
- [10] T. Q. Xiao, A. Bergamaschi, D. Dreossi, R. Longo, A. Olivo, S. Pani, L. Rigon, T. Rokvic, C. Venanzi, and E. Castelli, “Effect of spatial coherence on application of in-line phase contrast imaging to synchrotron radiation mammography,” *Nucl. Instr. and Meth. Phys. Res. B*, vol. 548, no. 1-2, pp. 155–162, Aug. 2005.

1 Introduction

Over the last two decades, various X-ray phase imaging methods have been studied and many applications have been developed. Phase-contrast images have delivered detailed images of the internal structures of samples consisting of weak absorption material such as biological and polymeric materials [1, 2]. Currently available techniques are classified by the method of phase retrieval used: grating-based (Talbot) differential phase-contrast imaging [3, 4], in-line phase-contrast imaging [5, 6], and diffraction enhanced imaging [7, 8].

Many of the previous experiments were carried out using a highly coherent and monochromatic X-ray from a synchrotron radiation. Alternative methods—partial coherent and polychromatic low-brilliance X-rays—have been used on grating-based phase-contrast imaging [2, 3]. The principle of the X-ray grating interferometer is the same as that of the visible light Talbot interferometer, but with the fabrication of gratings and operations with low-brilliance and an incoherent X-ray source, it is challenging to realize X-ray phase imaging in many applications. In order to meet the system requirements of X-ray phase imaging, a high brilliance X-ray source is the principle specification because of the high absorption loss of X-rays by air and grating. In our experiment, a 2-dimensional self-standing square grating is used as the source grating in order to fulfill the postulations of brilliance and coherence. Two other gratings also form a grating without a substrate. The configuration of grating is basically in-line phase imaging and phase detection implemented in a phase stepping method.

In this paper, a novel X-ray grating interferometer with partial coherent polychromatic is described, and then the results of X-ray phase imaging using a conventional low-brilliance X-ray tube on the wrapped phase-map images of an IC chip under packaging will be reported.

2 Methods

There are three gratings in the phase imaging set-up: source grating G_0 , a beam splitter grating G_1 , and an analyzer grating G_2 . X-ray grating differential phase-contrast imaging is based the self-imaging phenomenon of a periodic object. A periodic pattern, i.e., self-images, is generated by a beam splitting grating at the specific distance of np^2/λ , called the Talbot distance z_t , where p is the period of the grating, λ is the wavelength of the X-rays, and n is the Talbot integer. The Moiré fringe pattern is observed behind the analyzer grating, which is placed at the Talbot distance. The intensity of the Moiré fringe pattern is given by:

$$I(x, y) = I_0 a_0 + 2I_0 \sum_{n \geq 1} a_n \cos \left[2\pi \frac{n}{d} (z_t \varphi(x, y) + k) \right], \quad (1)$$

where I_0 is the intensity of the incident X-rays, k is the displacement of the analyzer grating in the distance of its pitch, a_n is the Fourier coefficient—which is determined by the grating and the spatial coherence—and $\varphi(x, y)$ is the beam deflection angle caused by the differential phase shift by an object:

$$\varphi(x, y) = \frac{\lambda}{2\pi} \frac{\partial \Phi(x, y)}{\partial x}. \quad (2)$$

The distance between the source grating and the beam splitter is chosen as the interference pattern of source grating created by neighboring virtual sources. The relationship between the distance from the source grating and the grating G_1 is given by:

$$l = \left(\frac{n}{2\lambda} \right) \frac{p_0^2 p_2}{p_0 + p_2}, \quad (3)$$

where n is the fractional Talbot distance and p_0 and p_2 are periods of G_0 and G_2 , respectively. The source is partially coherent in exhibiting phase contrast. The partial coherence is specified in terms of the lateral coherence length L_l [9]:

$$L_l = \frac{\lambda l_0}{s}, \quad (4)$$

where l_0 is the distance from the source to object and s is the source size.

3 Results and discussion

The X-ray phase imaging experiment involves a laboratory X-ray tube, three gratings, and an image detector device. The X-ray generator used for the experiment was a Spellman DF-8 with a copper (Cu) line focus tube operated at 45.3 kV and 8.0 mA. Figure 1 shows the X-ray phase imaging set-up with a standard X-ray tube and three transmission gratings. The periods of gratings are $p_0 = 12.5 \mu\text{m}$ with a $7.5 \mu\text{m}$ wide opening for the source grating, and both p_1 and $p_2 = 63 \mu\text{m}$ ($42 \mu\text{m}$ opening). A square type of source grating made from gold (Au) is mounted on the front of the X-ray tube exit aperture.

The distance between the source grating G_0 , and the beam splitter grating G_1 is $l = 6.5 \times 10^{-2} \text{ m}$, and the length from G_1 to G_2 is $d = 5 \times 10^{-3} \text{ m}$.

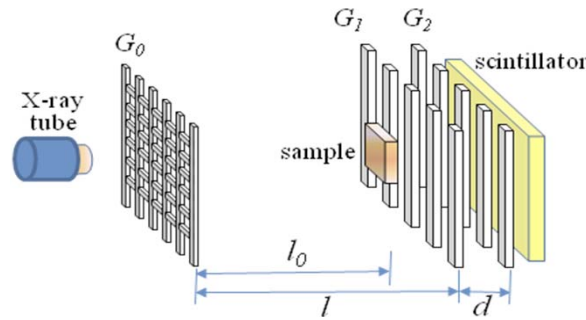


Fig. 1. X-ray phase imaging set-up with a standard X-ray tube and three transmission gratings.

A single crystal of YAG:Ce as a scintillator and a cooled charge-coupled device (CCD) are included in the image detector. A $150\text{ }\mu\text{m}$ thick scintillator screen is mounted on the back side of grating G_2 , followed by the CCD attached on the magnifying microscopy. The object needs to be an extremely long distance from the source in the conventional set-up of an X-ray Talbot interferometer [10]. In the case of a laboratory X-ray source, this distance l is not feasible in many practical applications. We employ X-ray 8.0 keV with a source size of $7.5\text{ }\mu\text{m}$; thus, $l = 16.7 \times 10^{-2}\text{ m}$ as obtained by Eq. (1). In our experiment, $l = 6.5 \times 10^{-2}\text{ m}$, and the distance l_0 from the source to the object is $6.0 \times 10^{-2}\text{ m}$. Therefore, a lateral coherence length L_l of $1.2\text{ }\mu\text{m}$ can be achieved in our configuration. The set-up parameters in our interferometer may not be appropriated for the conventional grating interferometer. However, Xu and Liu examined the claim that the lateral coherence length L_l and the shearing length $L_s (= \lambda d|u|/M)$ contribute to phase-contrast visibility [9]. When the ratio of the shearing length and the lateral coherence L_s/L_l is less than one, the X-ray waves are fully coherent over the shearing length and the phase contrast associated with this structure component is visible. For intermediate cases with $L_s/L_l < 1$, the X-ray is partially coherent and the phase contrast visibility increases with the decrease of the shearing length. In our X-ray interferometer configuration, the ratio $L_s/L_l \approx 0.1$ with $d = 5 \times 10^{-3}\text{ m}$, the spatial frequency of the structural component of the object $u = 1.43 \times 10^5$, and the magnification $M \approx 1.01$ provide a measure of the coherence degree that is realized in phase imaging.

An IC chip (TOSHIBA, TC4030BP) is used as a sample under packaging condition. X-ray imaging is performed with the sample placed at $5 \times 10^{-3}\text{ m}$

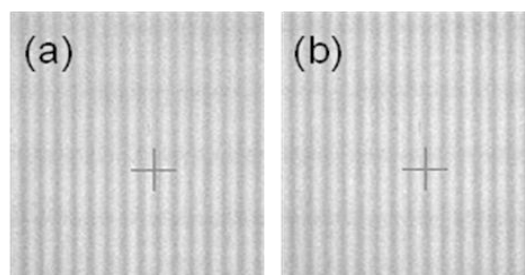


Fig. 2. Moiré fringes without an IC chip.

in front of the beam splitter grating G1. The phase information is acquired by a phase stepping method in which the analyzer grating is scanned along the periodical direction of the beam splitter grating. The intensity variation of the Moiré fringes given by Eq. (1) is visualized without an object for the first scan (a) and the fifth scan (b), as shown in Fig. 2. Scans were performed while the cross marks as reference points on the microscopy are fixed at the point. An absorption image of the packaged IC chip is shown in Fig. 3 (a); the image was taken with an exposure time of 34 msec. The same exposure time was used in each step of scanning. The wrapped phase map of the section in the absorption image is shown in Fig. 3 (b).

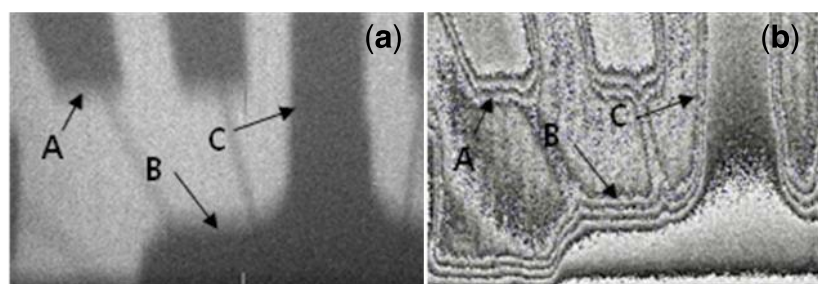


Fig. 3. An absorption image (a) and a wrapped phase map image (b) of a section of a packaged IC chip.

The IC chip sample is slightly leaned with its top side toward the beam splitter grating; areas A and B of Fig. 3 are on the sidewall of the component. A narrow sidewall can be seen in area C, when compared with areas A and B. Thus, the slope is much steeper in area C than in areas A and B. The slope of the sidewall or the degree of the tilting angle of the sample can be easily identified by a wrapped phase image (Fig. 3 (b)). The thickness of area A is about $250\ \mu\text{m}$, which is equal to 4 phase changes, and the thickness of area B is $315\ \mu\text{m}$, which is equivalent to 5 phase changes.

4 Conclusions

The new X-ray grating interferometer configuration that we have presented in this paper is compact and accessible and can be used for phase imaging with a polychromatic partial coherence X-ray source. The requirement of beam coherence and brilliance are modulated by using a free standing square source grating with a low brilliance laboratory X-ray source.

The details of the internal structure of packaged IC chip are revealed and the reconstruction of its wrap phase map is achieved. The results show that our configuration provides an alternative approach to obtaining a phase image for use in a wide range of applications in material science, nondestructive testing, and medical diagnostics. In addition, the X-ray grating interferometer can detect very small wave front distortions, making it useful for imaging electro-optic devices and microelectromechanical systems (MEMS), which are embedded inside opaque packaging.

Acknowledgments

This work was supported by the National Research Foundation of Korea (NRF) grant funded by the Korea government (MEST) (No. 2008-2003951).